DOI: 10.1002/chem.200601653

Highly Interpenetrated Supramolecular Networks Supported by N···I Halogen Bonding

Pierangelo Metrangolo,*[a] Franck Meyer,[a] Tullio Pilati,[b] Davide M. Proserpio,[c] and Giuseppe Resnati*[a]

Abstract: Halogen bonding (XB) has been used to assemble tetrakis(4-pyridyl)pentaerythritol (tetradentate XB acceptor) with different α,ω-diiodoperfluoroalkanes (bidentate XB donors) or tetrakis(4-iodotetrafluorophenyl)-pentaerythritol (tetradentate XB donor). The remarkable linearity of the XB formed, the rodlike character of α,ω-diiodoperfluoroalkanes and the mutual complementarities of pentaerythritol partners, translate the three-dimensional character of the XB acceptor into open primary networks, which interpenetrate to avoid the presence of voids and to ensure segregation of the modules. Two-dimensional (2D) square 4^4 layers (**sql**) with fourfold and fivefold interpenetration, as well as an eightfold diamondoid network (**dia**) of class Ia and a remarkable tenfold **dia** network of class IIIa, have been obtained.

Keywords: halogen bonds · interpenetrated networks · self-assembly · supramolecular chemistry · topology

Introduction

The structure of a crystal can seldom be anticipated with any degree of confidence from the structure of its constituent molecules,[1] and this becomes an even more remote possibility in the case of multicomponent heteromeric crystals. The aim of the strategy of molecular tectonics[2] is to create supramolecular constructions by design, which may be helpful in the realm of crystal engineering. Molecular tectonics is based on the use of special molecules, called tectons,[3] the molecular structures and intermolecular recognition features of which favour predictable self-assembly processes. Tectons consist of "sticky sites", which direct molecular association and encode a specific assembling algorithm. These sticky sites are pre-organised in well-defined orientations by a conformationally rigid scaffold.

Halogen bonding (XB) denotes non-covalent interactions involving halogens as electrophilic sites.[4] Despite the seminal studies by O. Hassel in the 1950s and his Nobel Lecture in 1969,[5] the relevance of the interaction was undervalued for a long time. In the late 1990s, we demonstrated the effectiveness of XB in crystal engineering,[6] and these studies prompted a renewed interest in the potential of the interaction in many other fields,[7] most notably in drug–receptor interactions,[8] supramolecular organic conductors,[9] and liquid crystals.[10] Iodoperfluorocarbons (iodo-PFC) proved to be particularly effective XB donors by virtue of the high polarisability of iodine and the ability of fluorine to boost the electron-acceptor potential of iodine atoms in the same molecule. Diiodo-PFCs are very reliable tectons, and this also holds for long-chain α,ω-diiodoperfluoroalkanes. Fluorination suppresses alkyl-chain flexibility so that α,ω-diiodoperfluoroalkanes behave as rigid rods, in which the "sticky sites" are the terminal iodine atoms and the number of difluoromethylene units predictably determines the separation between these sites. A major component of XB is frequently an $n \rightarrow \sigma^*$ donation, namely a transfer of electron density from an occupied non-bonding orbital of the electron donor atom (XB acceptor) to the vacant C–halogen antibonding

[a] Prof. Dr. P. Metrangolo, Dr. F. Meyer, Prof. Dr. G. Resnati
NFMLab c/o Department of Chemistry, Materials, and Chemical Engineering "Giulio Natta", Politecnico di Milano
7, via Mancinelli, 20131 Milan (Italy)
and
Campus of Como, Politecnico di Milano
Via Castelnuovo 7, 22100 Como (Italy)
Fax: (+39) 02-2399-3080
E-mail: pierangelo.metrangolo@polimi.it
giuseppe.resnati@polimi.it

[b] Dr. T. Pilati
CNR–Institute of Molecular Science and Technology
University of Milan
19, via Golgi, 20133 Milan (Italy)

[c] Prof. Dr. D. M. Proserpio
Department of Structural Chemistry and Inorganic Stereochemistry
University of Milan
21, via Venezian, 20133 Milan (Italy)

orbital of the electron-acceptor atom (XB donor). Consistent with this rationalisation, XB leads to an extension of the C–halogen covalent bond, and the stronger the XB, the more linear the arrangement.

We reasoned that if α,ω-diiodoperfluoroalkanes were to self-assemble with polydentate, three-dimensional XB acceptors, the remarkable linearity of the XB formed and the rodlike character of α,ω-diiodoperfluoroalkanes might translate the three-dimensional character of the XB acceptor into open primary networks, in which significant empty space would be created in the form of large channels, cavities or voids. In order to avoid collapse of the crystal lattice, these large spaces would need to be filled, which might be achieved either by the formation of solvent clathrates or by interpenetration of the networks.[11] We report herein that interpenetration does indeed occur when 1,4-diiodoperfluorobutane (**2**), 1,6-diiodoperfluorohexane (**3**) and 1,8-diiodoperfluorooctane (**4**) self-assemble through XB with tetrakis(4-pyridyloxymethylene)methane (**1**) (Scheme 1).

As expected, the pentaerythritol derivative **1** behaves as a tetradentate XB acceptor, while the diiodoperfluoroalkanes **2**, **3** and **4** serve as bidentate XB donors. The networks formed, **6**, **7** and **8**, respectively, thus show a 1:2 ratio of the XB-acceptor and -donor modules and present different topologies of complex interpenetration. A rare diamondoid eightfold network (**dia**) of class Ia[12] is shown by **6** (Scheme 2), while two-dimensional (2D) square 4^4 layers

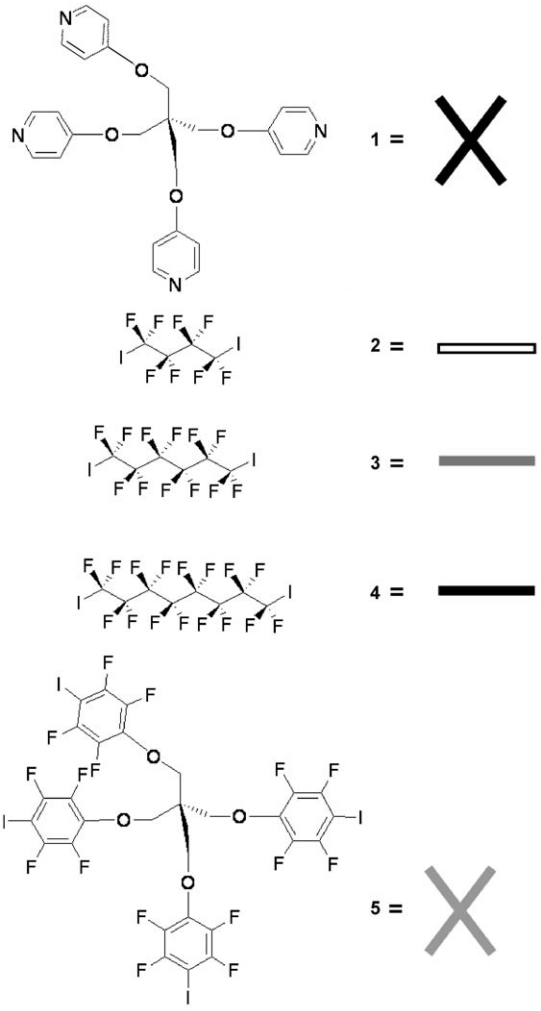

Scheme 1. Modules involved in the self-assembly processes.

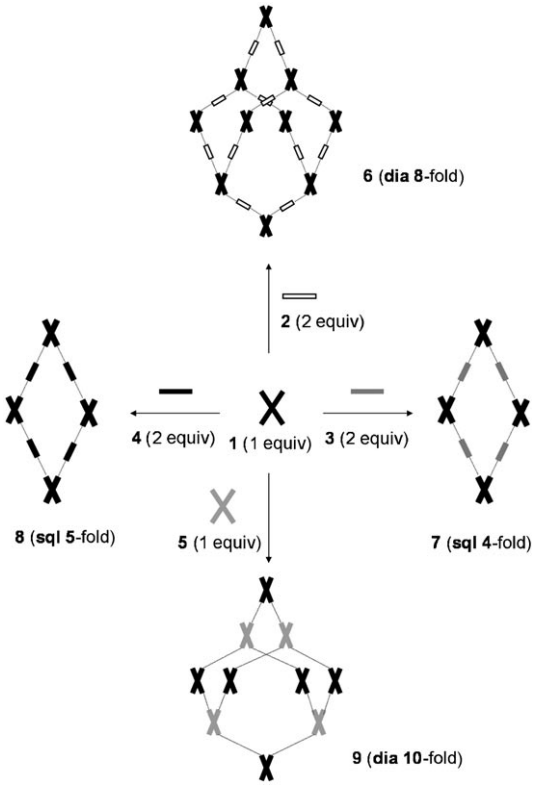

Scheme 2. Formation of halogen-bonded supramolecular complexes **6**–**9** through the self-assembly of modules **1**–**5**.

(**sql**) with fourfold and fivefold interpenetration are seen in **7** and **8**. We also self-assembled tetrapyridylpentaerythritol **1** with tetrakis(4-iodotetrafluorophenyloxymethylene)methane (**5**). Both XB-donor **5** and XB-acceptor **1** behave as tetradentate modules and are thus present in a 1:1 ratio in the resulting network **9**. In this adduct, a self-induced fitting process forces both modules to assume perfectly tetrahedral conformations, which results in the formation of a remarkable tenfold **dia** network of class IIIa.[12]

Results and Discussion

Pentaerythritol (**10**) is an inexpensive and readily available compound as it is widely used in industry for the synthesis of resins, surfactants and explosives.[13] Recently, it has been used to modulate metal chelation processes,[14] to tune the biological activity of multicomponent systems,[15] and to generate receptor-like libraries.[16] Tetradentate tectons[17] with a rigid tetrahedral core have been frequently employed in

supramolecular chemistry as their molecular topology is easily translated into a similar topology of the resulting supramolecular architectures. For instance, tetraphenylmethane and tetraphenylsilane derivatives have been used in hydrogen-bonding-driven formation of diamondoid networks or related three-dimensional, four-coordinated architectures.

Carbon tetrabromide is the simplest tetradentate XB-based tecton, and more complex modules have also been reported to afford diamondoid nets.[18] In contrast, pentaerythritol derivatives have received only occasional attention in supramolecular chemistry,[19] possibly because of the difficulty in anticipating the topology of the supramolecular architectures they may form. Indeed, the flexibility of the oxymethylene spacer, which bridges the tetrahedral core and the sticky sites appended to the oxygen atoms, prevents a straightforward prediction. This lack of an encoded bias towards a specific supramolecular structure was advantageous for our aim to test the ability of XB-driven self-assembly with diiodo-PFCs to give rise to interpenetrated networks. A pyridine nitrogen atom is known to serve as an effective XB-acceptor site and we thus prepared tetrakis(4-pyridyloxymethylene)methane (**1**) as a tetradentate XB-acceptor module.

Synthesis of pentaerythritol derivatives 1 and 5: Both pentaerythritol ethers **1** and **5** were prepared by nucleophilic aromatic substitution of the pentaerythritol alcoholate on the appropriate haloarene (Scheme 3).[20] This procedure gave

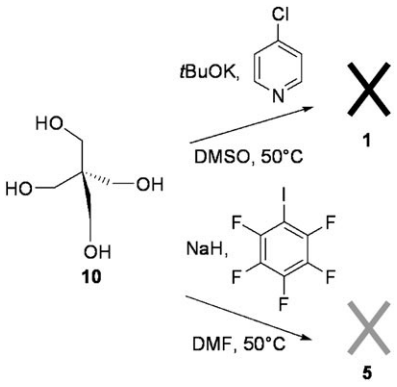

Scheme 3. Synthesis of tetrakis(4-pyridyl)pentaerythritol (**1**) and pentaerythritol tetrakis(2,3,5,6-tetrafluoro-4-iodophenyl) ether (**5**).

higher yields than nucleophilic substitution of the corresponding phenolate on pentaerythritol tetrabromide or tetratosylate.[21] Specifically, tetrakis(4-pyridyl)pentaerythritol (**1**) was obtained in 90% yield when pentaerythritol (**10**) was reacted with an excess of 4-chloropyridine in the presence of *t*BuOK in DMSO at 50°C. Tetrakis(4-iodotetrafluorophenyl)pentaerythritol (**5**) was isolated in 87% yield when pentaerythritol (**10**) was reacted with pentafluoroiodobenzene (PFIB) and NaH in DMF.

Crystal formation and structural analysis: Single crystals of adducts **6**–**9** were grown by isothermal evaporation of the solvent from ethanolic solutions of tetrapyridyl ether **1** containing either two equivalents of diiodo-PFCs **2**–**4** or one equivalent of tetrakis(iodophenyl) ether **5**. The ratios of the starting modules in the batch solids were determined by $^{1}H/^{19}F$ NMR analyses in the presence of bis(2,2,2-trifluoroethyl) ether as an internal standard.

The melting points of adducts **6**–**9** were found to be consistently higher than those of the pure fluorinated precursors **2**–**5**. Remarkably, the melting point of adduct **9** (226°C), which is 50°C higher than that of pure fluorocarbon precursor **5**, is also 28°C higher than that of pure hydrocarbon precursor **1**. The melting point of a substance depends on the strength of the intermolecular interactions and this dependence cannot be easily quantified due to the numerous parameters affecting the crystal packing. Nevertheless, this thermal behaviour is a simple but forceful indication that specific and relatively strong intermolecular interactions develop in adducts **6**–**9** and supports the presence of well-defined crystal species upon interaction of **1** with precursors **2**–**5**.

IR spectroscopy identifies the sticky sites on starting modules **1**–**5**. The spectra of the adducts **6**–**9** are approximately the sum of the spectra of the precursors; the band shifts and intensity changes as compared with the spectra of the pure starting modules are perfectly consistent with electron donation from the nitrogen atoms in **1** to the iodine atoms in **2**–**5**. As an inevitable consequence of the $n\rightarrow\sigma^*$ nature of the XB connecting the modules,[22] some bands of the electron-donor species **1** are blueshifted while some bands of the electron-acceptor modules **2**–**5** are redshifted upon adduct formation. For instance, the $\tilde{\nu}_{C\text{-}H}$ absorption of pure tetrapyridyl pentaerythritol **1** at 3025 cm^{-1} becomes less intense in adducts **6**–**9** and is shifted to 3041–3044 cm^{-1} in adducts **6**–**8** and to 3035 cm^{-1} in **9**. These variations are consistent with an increased positive charge on the H atoms in crystals **6**–**9** as compared to pure precursor **1**. As far as the electron-acceptor modules are concerned, the $\tilde{\nu}_{C\text{-}F}$ bands of diiodo-perfluorobutane **2** at 1195 and 1140 cm^{-1} are shifted to 1179 and 1124 cm^{-1} in adduct **6**; the $\nu_{C\text{-}F}$ bands of compound **3** at 1200 and 1142 cm^{-1} are redshifted to 1195 and 1138 cm^{-1} in **7**; and the bands at 642 and 556 cm^{-1} of pure **5**, associated with the C–I bond, are shifted to 620 and 545 cm^{-1}, respectively, in adduct **9**. Finally, the stretching absorption of the tetrafluorobenzene rings at 1487 cm^{-1} in pure **5** is redshifted to 1484 cm^{-1} in **9**.

Single-crystal X-ray analyses of adducts **6**–**9** give detailed structural information on both the conformation of the modules and the overall crystal packing.[23] Some of the modules lie on a crystallographic element of symmetry, as indicated in Figure 1, which shows the conformations of all of the modules in the supramolecular assemblies **6**–**9**.

Perfluoroalkyl chains usually adopt helically distorted all-*trans* conformations but, surprisingly, the perfluorobutyl chain of **2** assumes the quite rare *gauche* conformation in adduct **6** (Figure 1). As is usual for perfluoroalkyl chains,

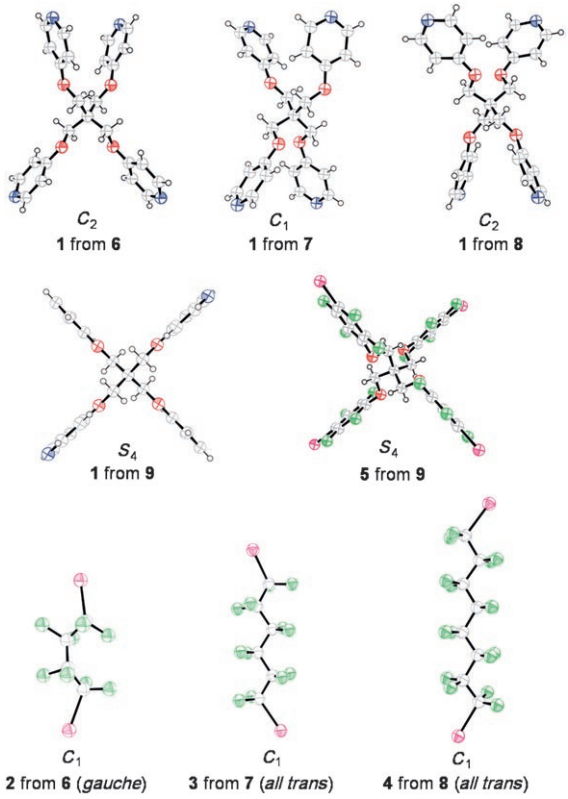

Figure 1. Conformations adopted by starting modules **1**–**5** in the supramolecular architectures **6**–**9**. Modules **2** (in **6**) and **4** (in **8**) are disordered; only one of the conformations adopted by these modules is reported here for the sake of simplicity. The crystallographic symmetries of the modules are also indicated; **1** (in **9**) is nearly D_{2d}, with root mean square (rms) of 0.0388.

both the perfluorobutyl chain of **2** and the perfluorooctyl chain of **4** show rotational disorder about the chain axis in the corresponding adducts **6** and **8**; two conformations, having the same population factor but opposite torsion angles along the chain, are present. In contrast, the perfluorohexyl chain of **3** shows no disorder and this may be related to the particularly compact architecture of the crystal **7**, as reflected in its high density.

A quantitative and concise bi-dimensional descriptor of the conformational variability of the pentaerythritol modules **1** and **5** is shown in Figure 2. In this diagram, the coordinates of a generic point $P(x,y)$ correspond to the ratios $x_i = I_{3i}/I_{2i}$ and $y_i = I_{1i}/I_{2i}$, in which $I_{3i} > I_{2i} > I_{1i}$ are the autovalues of the ellipsoids of inertia moments of the module i. In such a diagram, the points (1,1), (1,0) and (2,1) correspond to objects with the symmetry of a sphere, a line and a disc, respectively; the axes (1,y) and (x,1) represent a sphere that is stretched (prolate) or compressed (oblate) along a diameter, respectively. The black dots in the diagram indicate the conformations of tetrapyridyl-pentaerythritol **1** in adducts **6**–**9**, and the white dots indicate the conformations of tetrakis(iodophenyl)pentaerythritol **5** in adduct **9** and in the adducts **11** and **12** that it forms with (*E*)-1,2-di(4-pyridyl)ethylene and 1,2-diaminoethane, respectively.[6h]

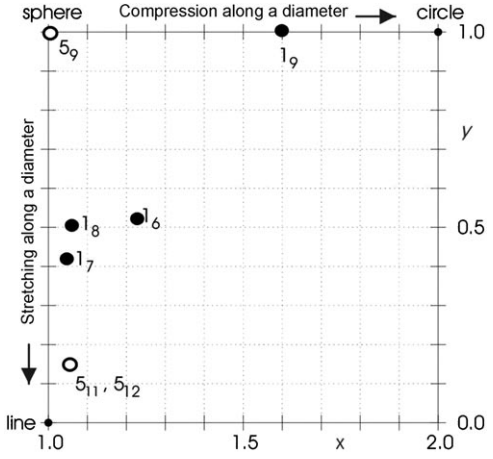

Figure 2. Diagram displaying the ratios $x_i = I_{3i}/I_{2i}$ and $y = I_{1i}/I_{2i}$ for the pentaerythritol derivatives **1** and **5** in the supramolecular architectures **6**–**9**, and in **11** and **12.** In the generic dot label $\mathbf{M_N}$, **M** is the pentaerythritol module and **N** is the adduct in which it is incorporated (e.g., the label $\mathbf{5_9}$ denotes the dot indicating the conformation adopted by tetrakis(4-iodophenyl)pentaerythritol **5** in adduct **9**).

Clearly, the pentaerythritol derivatives **1** and **5** do not have a conformation that is much more favoured than the others from an energetic point of view. By virtue of the flexibility of the oxymethylene spacer bridging the tetrahedral core and the nitrogen and iodine atoms at the periphery of the modules, the conformation that these modules adopt changes according to the partner with which they interact. Conformational adaptation occurs in order to maximise the matching of the complementary modules and the stability of the overall crystal packing. The mesogenic character of perfluoroalkyl chains and the remarkable directionality of XB result in the formation of highly open networks, in which interpenetration allows the voids to be filled and ensures segregation of the modules (necessitated, in adducts **6**–**8**, by the low affinity of perfluoroalkyl chains for hydrocarbon derivatives) (Figure 3).

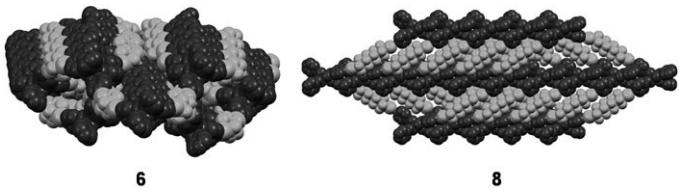

Figure 3. Spacefill view of the crystal packing in complexes **6** (left) and **8** (right) showing the segregation between HC (black) and PFC (grey) modules.

Description of the interpenetration: The supramolecular networks **7** and **8** are organised in 2D square layers (**sql**) with 4^4 topology.[12] These supramolecular arrangements are comprised of four- and fivefold interpenetrated **sql** that share the same average plane (Figure 4).[24]

The modules are connected by N···I halogen bonds, which transfer topological information through the polymeric

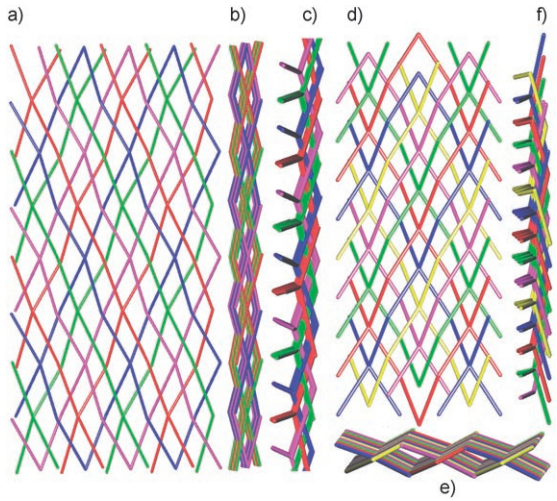

Figure 4. Schematic views of the interpenetrated square layers observed in fourfold **7** (a, b, c) and fivefold **8** (d, e, f). The rhombic mesh is visible in views (a) and (d) down [0,0,1], the normal to the common average plane of the layers. The lateral views ([1,0,0] and [1,1,0] for (b) and (c), [0,1,0] and [1,5,0] for (e) and (f)) reveal the different interpenetration class types: class Ia with a unique translational vector [0,1,0] for **8**; class IIIa [2×2] for **7**.

chains. The undulated layers are formed of rhombic units with side lengths of 26.61 and 29.61 Å in **7** and **8**, respectively, consistent with a longer fluorinated chain in **8**. In compound **7**, the N···I distances are in the range 2.72–2.75 Å (approximately 23% shorter than the sum of the van der Waals radii) and the N···I–C angles are almost linear (170–178°). The crystallographic data for **8** revealed the interactions to be somewhat weaker in this case, with distances in the range 2.84–2.86 Å and the N···I–C angles in the range 160–176°. Extending the classification of 3D interpenetrated arrays[12] to the 2D **sql** observed in **7** and **8**, we find that the nodes of the five **sql** in **8** are related by a simple translation with the shortest interpenetration vector [010] of 10.4775(8) Å, thus conforming to class Ia (interpenetration of *n*-fold nets with *n* = prime number > 3 can only be of class Ia[12b]). In contrast, the four **sql** in compound **7** belong to class IIIa, with a combination of the [1,0,0] translation (10.59 Å) and a 2_1 screw axis. In both cases, the layers share the same average plane (Figure 4b, e), but the wavy sheets in **7** are organised in alternating pairs that show 2×2 = 4-fold interpenetration of class IIIa type (Figure 4c). The resulting entangled systems exhibit a degree of interpenetration that ranks among the highest seen for **sql** networks and, remarkably, no fourfold **sql** and only one fivefold (also of class Ia) are reported in the extensive database compiled by Batten.[25]

According to the results reported above, the XB-driven formation of highly interpenetrated systems with the shorter diiodoperfluorobutane module **2** is seemingly a compromised pathway. However, the self-assembly of starting modules **1** and **2** provided the unexpected eightfold interpenetrated network **6**. From a topological point of view,[26] the basic unit is a diamondoid cage, which is the elementary design of highly interpenetrated networks;[12a] a single motif is illustrated in Figure 5 (left). Indeed, this pattern ensures that the large cavities are mainly filled by other interpenetrating nets. The starting modules are linked by N···I bonds with distances of 2.80–2.87 Å and N···I–C angles of 166–177°, giving rise to a highly distorted diamondoid cage that exhibits maximum dimensions (corresponding to the longest intracage distances between the tetraconnected nodes) of $2a \times 2b \times 4c$ (i.e., 20.03×40.40×87.86 Å).

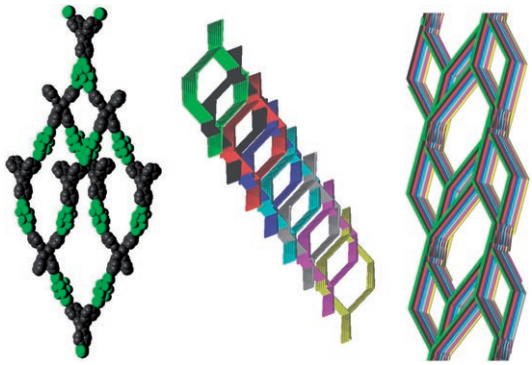

Figure 5. Molecular structure of the diamondoid cage of complex **6** (left); schematic view of a set of eight diamondoid cages with the interpenetration vector [½,½,½] (centre); overall view of the eightfold interpenetrated networks (right).

This structure exhibits an eightfold interpenetration, a rare interpenetration for exclusively organic molecules. The eight interpenetrated diamondoid arrays are related by a single interpenetration vector corresponding to a half body diagonal [½,½,½] of 15.74 Å and are thus of class Ia type. The interpenetration direction is also not "normal", that is, it is not parallel to one of the "ideal" twofold axes of the adamantoid cage as observed in a few cases (see ref. [26b] for details, in particular the eightfold **dia** of [Ag(dodecanedinitrile)$_2$]AsF_6).

Finally, the supramolecular network **9** exhibits one of the highest degrees of **dia** interpenetration reported to date, the highest being 11-fold, as observed in a hydrogen-bonded supramolecular network,[27] and tenfold, as observed for covalent networks.[26b] By virtue of the high directionality and selectivity of XB, self-assembly of the symmetric tetratopic modules **1** and **5** gives rise to a precise diamondoid network, the basic unit of which is represented in Figure 6 as a compressed adamantoid cage with maximum dimensions of 31.74×43.52×43.52 Å.

The relevance of XB in the coherence of the crystal structure of **9** is also revealed by the dramatic increase in its melting point (226–228 °C) compared with those of the pure starting modules **1** and **5** (198 °C and 166 °C, respectively). The strong interaction is also highlighted by an N···I distance that is close to 20% shorter than the sum of the van der Waals radii (2.82 Å) and an almost linear N···I–C angle (175°). Moreover, π–π stacking between the pyridyl and perfluoroarene rings also contributes to the packing of the modules in the crystal lattice (centroid–centroid distance 4.16 Å).

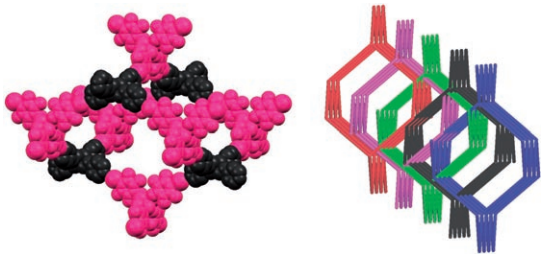

Figure 6. Molecular structure of the diamondoid cage of **9** made up of modules **1** and **5** (black and pink, respectively) (left); schematic view of a subset of five diamondoid cages, with the translational interpenetration vector [1,0,0], that form the tenfold network (right).

From the topological point of view, this structure is characterised by a mode of interpenetration belonging to class IIIa.[12] The characteristic feature of this mode is the presence of both translational vectors and non-translational symmetry elements, which relate the individual sub-nets in two sets.

Five nets are related by the translating interpenetration vector [1,0,0] (or its equivalent [0,1,0] imposed by the tetragonal symmetry) with a repeat distance between the nets of 13.76 Å, as illustrated in Figure 6; five **dia** nets are superimposed along the cell axis *a* (and equivalently along *b*). The presence of an interpenetration symmetry element as the inversion centre generates a second set of five **dia** nets for a total degree of interpenetration of class IIIa of $10=[5\times2]$ (Figure 7). This is the highest degree of interpenetration hitherto reported for class IIIa.

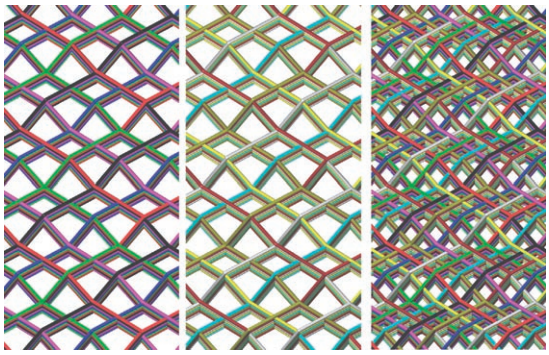

Figure 7. Schematic view of the two different fivefold networks of **9** (with translating interpenetration vectors [1,0,0] and [0,1,0]) (left and centre) that combine through the inversion centre to give the overall 10[5×2]-fold interpenetration of class IIIa (right).

Conclusions

In conclusion, we have reported the formation of halogen-bonded interpenetrated networks with three different types of topology. Compounds **7** and **8** are characterised by 2D square 4^4 networks with degrees of interpenetration of four and five. XB is also responsible for the self-assembly of an eightfold diamondoid network **6** with a topological type belonging to class Ia. Finally, the framework **9** exhibits the unusual mode of interpenetration of **dia** class IIIa, with the second highest degree of interpenetration described to date, namely a tenfold topology. Only a small number of interpenetrated networks based on XB have hitherto been reported.[16,18] The results described in this paper clearly demonstrate that XB coupled with the use of diiodoperfluoroalkanes offers a reliable means of constructing complex interpenetrated structures by design.

Experimental Section

General methods: Commercial HPLC-grade solvents were used without further purification. Starting materials were purchased from Sigma-Aldrich, Acros Organics and Apollo Scientific. Reactions were carried out in oven-dried glassware under a nitrogen atmosphere. ^{1}H, ^{19}F and ^{13}C NMR spectra were recorded at ambient temperature on a Bruker AV500 spectrometer. Unless otherwise stated, $CDCl_3$ was used as both solvent and internal standard in acquiring ^{1}H and ^{13}C NMR spectra. In the case of ^{19}F NMR spectra, $CDCl_3$ was used as solvent and $CFCl_3$ as internal standard. All chemical shift values are given in ppm. IR spectra were obtained from samples in KBr pellets using a Perkin–Elmer 2000 FTIR spectrometer. Absorptions are specified in wavenumbers, which have been rounded to the nearest 1 cm^{-1} by automatic assignment. Selected IR data of the starting modules are reported to show the changes that occur upon the formation of co-crystals **6**–**9**. Mass spectra were recorded with a Finnigan Mod TSQ-70 instrument in FAB mode from an *m*NBA matrix. Mass-to-charge ratios and relative intensities (%) with respect to the parent ions are given. Melting points were determined with a Reichert instrument by observing the melting and crystallising processes through an optical microscope.

Single-crystal X-ray analyses: Data were collected with a Bruker APEX CCD area detector diffractometer equipped with an Oxford low-temperature device using graphite-monochromated $Mo_{K\alpha}$ radiation ($\lambda=0.71069$ Å); ω and ϕ scans; data collection and data reduction were performed with the SMART and SAINT program packages; an absorption correction, based on a multi-scan procedure, was applied using SADABS.[28] Data for **6**, **8** and **9** were collected at room temperature, whereas those for **7** were collected at 123 K (Table 1). The structures were solved using SIR2002,[29] and refined on all independent reflections by full-matrix least-squares based on F_o^2 using SHELX-97.[30] The disordered -$(CF_2)_n$- chains of **6** and **8** were refined with restraints on both atomic distances and anisotropic displacement parameters. H atoms in all structures were placed in calculated positions. Further crystallographic details of the structures reported in this paper, not presented in Table 1, have been deposited with the Cambridge Crystallographic Data Centre. CCDC-625929 (**6**), -625931 (**7**), -625930 (**8**) and -625928 (**9**) contain the supplementary crystallographic data for this paper. These data can be obtained free of charge from the Cambridge Crystallographic Data Centre via www.ccdc.cam.ac.uk/data_request/cif.

Synthesis of tetrakis(4-pyridyl)pentaerythritol (1): Pentaerythritol (**10**, 68 mg, 0.5 mmol) and *t*BuOK (280 mg, 2.5 mmol) were stirred in DMSO (1 mL) at room temperature for 40 min. A solution of 4-chloropyridine (590 mg, 10.4 mmol) in DMSO (1 mL) was then slowly added and the reaction mixture was heated at 50 °C. After 24 h, saturated aqueous NaCl solution was added, the aqueous layer was extracted four times with CH_2Cl_2 and the combined organic layers were dried over Na_2SO_4. After evaporation of the solvent, the crude material was purified by column chromatography on silica gel (240–400 mesh), eluting with CH_2Cl_2/MeOH (2:1), to give the product in 90% yield. M.p. 198 °C; ^{1}H NMR: $\delta=4.47$ (s, 8H; CH_2), 6.80 (d, 8H, $J=6.4$ Hz; H arom.), 8.40 ppm (d, 8H, $J=6.4$ Hz; H arom.); IR: $\tilde{\nu}_{max}=3025$, 2944, 1598, 1504, 1464, 1424, 1278, 1214, 1025, 842, 816, 654 cm^{-1}.

Synthesis of pentaerythritol tetrakis(2,3,5,6-tetrafluoro-4-iodophenyl) ether (5): Pentaerythritol (**10**, 68 mg, 0.5 mmol) and NaH (90 mg,

Table 1. Selected crystallographic and data collection parameters for co-crystals **6–9**.

	6	**7**	**8**	**9**
molecular formula	$C_{25}H_{24}N_4O_4{\cdot}2\,(C_4F_8I_2)$	$C_{25}H_{24}N_4O_4{\cdot}2\,(C_6F_{12}I_2)$	$C_{25}H_{24}N_4O_4{\cdot}2\,(C_8F_{16}I_2)$	$C_{25}H_{24}N_4O_4{\cdot}C_{29}H_8F_{16}I_4O_4$
M_r	1352.16	1552.20	1752.24	1676.44
crystal colour	colourless	colourless	colourless	colourless
dimensions [mm]	$0.32\times0.18\times0.14$	$0.39\times0.16\times0.13$	$0.32\times0.26\times0.20$	$0.32\times0.20\times0.14$
T [K]	295(2)	123(2)	295(2)	295(2)
crystal system	orthorhombic	monoclinic	monoclinic	tetragonal
space group	*Iba*2	$P2_1/n$	*C*2/*c*	$I4_1/a$
a [Å]	10.0144(8)	10.5915(15)	27.599(2)	13.764(2)
b [Å]	20.202(2)	24.415(4)	10.4711(8)	–
c [Å]	21.964(2)	18.995(3)	20.195(2)	31.739(6)
β [°]	–	95.59(2)	101.97(2)	–
V [Å^3]	4443.6(7)	4888.6(13)	5709.3(8)	6012.9(17)
Z	4	4	4	4
ρ_{calcd} [g cm^{-1}]	2.021	2.109	2.039	1.852
$\mu(Mo_{K\alpha})$ [mm^{-1}]	2.912	2.684	2.330	2.177
T_{min}/T_{max}	0.800	0.728	0.860	0.877
$2\theta_{max}$ [°]	60.06	69.10	52.00	51.36
data collected	50407	133750	35616	45054
unique data, R_{int}	6135, 0.0365	20067, 0.0292	5607, 0.0253	2780, 0.0307
observed data [$I_o > 2\sigma(I_o)$]	4361	17307	3656	1703
parameters, restraints	402, 508	658, 0	600, 1074	194, 0
R_{all}, R_{obsd}	0.0591, 0.0365	0.0381, 0.0306	0.0754, 0.0502	0.0639, 0.0347
wR_{all}, wR_{obsd}	0.0888, 0.0791	0.0734, 0.0711	0.1518, 0.1339	0.0996, 0.0877
GOF	1.047	1.057	1.028	0.912
$\Delta\rho_{min,max}$ [e Å^{-3}]	−0.22, 0.44	−0.70, 2.29	−0.50, 1.16	−0.15, 0.45

4.5 mmol) were stirred in DMF (1.4 mL) at room temperature for 40 min. A solution of PFIB (0.48 mL, 8 mmol) in DMF (0.5 mL) was then slowly added at 0 °C and the reaction mixture was heated at 50 °C overnight. Thereafter, the solution was hydrolysed with water, the aqueous layer was extracted four times with CH_2Cl_2 and the combined organic layers were dried over Na_2SO_4. After evaporation of the solvent, the crude material was purified by column chromatography on silica gel (240–400 mesh), eluting with hexane/CH_2Cl_2 (95:5), to give the product in 87% yield. M.p. 166 °C; ^{1}H NMR: $\delta = 4.61$ ppm (s, 8H; CH_2); ^{13}C NMR: $\delta = 47.62$ (s; C), 65.28 (t, $J = 27$ Hz; C–I), 71.67 (s; CH_2), 147.70 (m; C–O), 140.64 (dm_c, $J = 251$ Hz; *ortho*-C), 147.48 ppm (dm_c, $J = 242$ Hz; *meta*-C); ^{19}F NMR: $\delta = -155.0$ (d, 8F, $J = 16$ Hz; OCCF), −120.9 ppm (d, 8F, $J = 16$ Hz; ICCF); IR: $\tilde{\nu}_{max} = 2968$, 1644, 1487, 1470, 1452, 1494, 1409, 1277, 1165, 1104, 991, 967, 944, 804 cm^{-1}; MS (FAB in *m*NBA): *m*/*z*: 1242 (40) {M$^{+\bullet}$}.

General procedure: Formation of co-crystals 6–9: Co-crystals **6–9** were obtained by dissolving one equivalent of tetrakis(4-pyridyl)pentaerythritol **1** and two equivalents of the respective perfluorodiiodoalkanes **2–4** (or equimolar amounts of pentaerythritol derivatives **1** and **5**) in ethanol at room temperature in a clear borosilicate glass vial. The open vial was placed in a closed cylindrical wide-mouth bottle containing Vaseline. The ethanol was allowed to diffuse at room temperature.

Co-crystal 6—Tetrakis(4-pyridyl)pentaerythritol (1) and perfluoro-1,4-diiodobutane (2): Colourless solid; m.p. 141–145 °C; IR: perfluoro-1,4-diiodobutane (**2**): $\tilde{\nu}_{max} = 1485$, 1195, 1140, 1089, 1042, 889, 764, 696, 646 cm^{-1}; co-crystal **6**: $\tilde{\nu}_{max} = 3041$, 2954, 1595, 1498, 1286, 1264, 1212, 1179, 1124, 1044, 1024, 996, 840, 821, 762, 649 cm^{-1}.

Co-crystal 7—Tetrakis(4-pyridyl)pentaerythritol (1) and perfluoro-1,6-diiodohexane (3): Colourless solid; m.p. 130 °C; IR: perfluoro-1,6-diiodohexane (**3**): $\tilde{\nu}_{max} = 1629$, 1200, 1142, 1087, 1048, 925 cm^{-1}; co-crystal **7**: $\tilde{\nu}_{max} = 3044$, 2954, 1593, 1502, 1281, 1207, 1195, 1138, 1112, 1080, 1042, 1024, 999, 816, 694 cm^{-1}.

Co-crystal 8—Tetrakis(4-pyridyl)pentaerythritol (1) and perfluoro-1,8-diiodooctane (4): Colourless solid; m.p. 130–140 °C; IR: perfluoro-1,8-diiodooctane (**4**): $\tilde{\nu}_{max} = 1207$, 1149, 1114, 1090, 1056, 845, 642, 556 cm^{-1}; co-crystal **8**: $\tilde{\nu}_{max} = 3043$, 2954, 1595, 1506, 1284, 1214, 1154, 1119, 1105, 1057, 875, 821, 620, 545 cm^{-1}.

Co-crystal 9—Tetrakis(4-pyridyl)pentaerythritol (1) and pentaerythritol tetrakis(2,3,5,6-tetrafluoro-4-iodophenyl) ether (5): Colourless solid; m.p. 226–228 °C; IR: $\tilde{\nu}_{max} = 3035$, 2956, 1599, 1484, 1480, 1284, 1246, 1210, 1096, 1042, 999, 970, 924, 842, 814, 799, 764 cm^{-1}.

Acknowledgements

We would like to thank the EU (D31/0017/05), the Fondazione Cariplo (Bandi aperti 2005-Progetti finalizzati al reclutamento di giovani ricercatori) and the European Office of Aerospace Research and Development (EOARD, contract FA8655-06-1-3040) for financial support.

[1] a) J. D. Dunitz, *Chem. Commun.* **2003**, *5*, 545; b) D. Braga, L. Brammer, N. R. Champness, *CrystEngComm* **2005**, *7*, 1.
[2] a) M. W. Hosseini, *CrystEngComm* **2004**, *6*, 318; b) D. Su, X. Wang, M. Simard, J. D. Wuest, *Supramol. Chem.* **1995**, *6*, 171; c) S. Mann, *Nature* **1993**, *365*, 499.
[3] a) M. Simard, D. Su, J. D. Wuest, *J. Am. Chem. Soc.* **1991**, *113*, 4696; b) P. Metrangolo, G. Resnati, "Tectons: Definition and Scope", in *Encyclopedia of Supramolecular Chemistry*, Marcel Dekker, New York, **2004**, p. 1484.
[4] a) P. Metrangolo, T. Pilati, G. Resnati, *CrystEngComm*, DOI: 10.1039/b610454a; P. Metrangolo, H. Neukirch, T. Pilati, G. Resnati, *Acc. Chem. Res.* **2005**, *38*, 386; b) P. Metrangolo, G. Resnati, "Halogen Bonding", in *Encyclopedia of Supramolecular Chemistry*, Marcel Dekker, New York, **2004**, p. 628; c) P. Metrangolo, G. Resnati, *Chem. Eur. J.* **2001**, *7*, 2511.
[5] O. Hassel, *Science* **1970**, *170*, 497.
[6] a) R. Liantonio, P. Metrangolo, F. Meyer, T. Pilati, W. Navarrini, G. Resnati, *Chem. Commun.* **2006**, 1819; b) A. Casnati, R. Liantonio, P. Metrangolo, G. Resnati, R. Ungano, F. Ugozzoli, *Angew. Chem.* **2006**, *118*, 1949; *Angew. Chem. Int. Ed.* **2006**, *45*, 1915; c) R. Bertani, E. Ghedini, M. Gleria, R. Liantonio, G. Marras, P. Metrangolo, F. Meyer, T. Pilati, G. Resnati, *CrystEngComm* **2005**, *7*, 511; d) H. Neukirch, E. Guido, R. Liantonio, P. Metrangolo, T. Pilati, G. Resnati, *Chem. Commun.* **2005**, 1534; e) A. Forni, P. Metrangolo, T.

Pilati, G. Resnati, *Cryst. Growth Des.* **2004**, *4*, 291; f) P. Metrangolo, T. Pilati, G. Resnati, A. Stevenazzi, *Chem. Commun.* **2004**, 1492; g) T. A. Logothetis, F. Meyer, P. Metrangolo, T. Pilati, G. Resnati, *New J. Chem.* **2004**, *28*, 760; h) T. Caronna, R. Liantonio, T. A. Logothetis, P. Metrangolo, T. Pilati, G. Resnati, *J. Am. Chem. Soc.* **2004**, *126*, 4500; i) R. Liantonio, P. Metrangolo, T. Pilati, G. Resnati, A. Stevenazzi, *Cryst. Growth Des.* **2003**, *3*, 799; j) R. Liantonio, P. Metrangolo, T. Pilati, G. Resnati, *Cryst. Growth Des.* **2003**, *3*, 355; k) A. De Santis, A. Forni, R. Liantonio, P. Metrangolo, T. Pilati, G. Resnati, *Chem. Eur. J.* **2003**, *9*, 3974; l) D. D. Burton, F. Fontana, P. Metrangolo, T. Pilati, G. Resnati, *Tetrahedron Lett.* **2003**, *44*, 645; m) R. Liantonio, S. Luzzati, P. Metrangolo, T. Pilati, G. Resnati, *Tetrahedron* **2002**, *58*, 4023; n) R. B. Walsh, C. W. Padgett, P. Metrangolo, G. Resnati, T. W. Hanks, W. T. Pennington, *Cryst. Growth Des.* **2001**, *1*, 165; o) W. Navarrini, P. Metrangolo, T. Pilati, G. Resnati, *New J. Chem.* **2000**, *24*, 777; p) M. T. Messina, P. Metrangolo, S. Pappalardo, M. F. Parisi, T. Pilati, G. Resnati, *Chem. Eur. J.* **2000**, *6*, 3495; q) E. Corradi, S. V. Meille, M. T. Messina, P. Metrangolo, G. Resnati, *Angew. Chem.* **2000**, *112*, 1852; *Angew. Chem. Int. Ed.* **2000**, *39*, 1782; r) V. Amico, S. V. Meille, E. Corradi, M. T. Messina, G. Resnati, *J. Am. Chem. Soc.* **1998**, *120*, 8261.

[7] a) A. Sun, J. W. Lauher, N. S. Goroff, *Science* **2006**, *312*, 1030; b) G. M. Espallargas, L. Brammer, P. Sherwood, *Angew. Chem.* **2006**, *118*, 449; *Angew. Chem. Int. Ed.* **2006**, *45*, 435; c) F. Zordan, L. Brammer, *Cryst. Growth Des.* **2006**, *6*, 1374; d) K. Boubekeur, J.-L. Syssa-Magalé, P. Palvadeauc, B. Schöllhorn, *Tetrahedron Lett.* **2006**, *47*, 1249; e) C. M. Reddy, M. T. Kirchner, R. C. Gundakaram, K. A. Padmanabhan, G. R. Desiraju, *Chem. Eur. J.* **2006**, *12*, 2222; f) S. V. Rosokha, I. S. Neretin, T. Y. Rosokha, J. Hecht, J. K. Kochi, *Heteroat. Chem.* **2006**, *17*, 449; g) F. Zordan, L. Brammer, P. Sherwood, *J. Am. Chem. Soc.* **2005**, *127*, 5979; h) T. Takeuchi, Y. Minato, M. Takase, H. Shinmoria, *Tetrahedron Lett.* **2005**, *46*, 9025; i) A. Mele, P. Metrangolo, H. Neukirch, T. Pilati, G. Resnati, *J. Am. Chem. Soc.* **2005**, *127*, 14972; j) B. K. Saha, A. Nangia, M. Jaskólski, *CrystEngComm* **2005**, *7*, 355; k) R. Bertani, P. Metrangolo, A. Moiana, E. Perez, T. Pilati, G. Resnati, I. Rico-Lattes, A. Sassi, *Adv. Mater.* **2002**, *14*, 1197; l) S. George, A. Nangia, C.-K. Lam, T. C. W. Mak, J.-F. Nicoud, *Chem. Commun.* **2004**, 1202; m) J. A. R. P. Sarma, F. H. Allen, V. J. Hoy, J. A. K. Howard, R. Thaimattam, K. Biradha, G. R. Desiraju, *Chem. Commun.* **1997**, 101; n) P. K. Thallapally, G. R. Desiraju, M. Bagieu-Beucher, R. Masse, C. Bourgogne, J.-F. Nicoud, *Chem. Commun.* **2002**, 1052; o) A. Farina, S. V. Meille, M. T. Messina, P. Metrangolo, G. Resnati, *Angew. Chem.* **1999**, *111*, 2585; *Angew. Chem. Int. Ed.* **1999**, *38*, 2433.

[8] a) Y. Jiang, A. A. Alcaraz, J.-M. Chen, H. Kobayashi, Y. J. Lu, J. P. Snyder, *J. Med. Chem.* **2006**, *49*, 1891; b) L. K. Steinrauf, J. A. Hamilton, B. C. Braden, J. R. Murrel, M. D. Benson, *J. Biol. Chem.* **1993**, *268*, 2425; c) M. Adler, M. J. Kochanny, B. Ye, G. Rumennik, D. R. Light, S. Biancalana, M. Whitlow, *Biochemistry* **2002**, *41*, 15514; d) P. Auffinger, F. A. Hays, E. Westhof, P. Shing Ho, *Proc. Natl. Acad. Sci. USA* **2004**, *101*, 16789; e) I. Saraogi, V. G. Vijay, S. Das, K. Sekar, T. N. Guru Row, *Cryst. Eng.* **2003**, *6*, 69.

[9] a) T. Imakubo, H. Sawa, R. Kato, *Synth. Met.* **1995**, *73*, 117; b) P. Batail, M. Fourmigué, *Chem. Rev.* **2004**, *104*, 5379; c) T. Imakubo, N. Tajima, M. Tamura, R. Kato, Y. Nishio, K. Kajita, *Synth. Met.* **2003**, *133*, 181.

[10] a) J. Xu, X. Liu, T. Lin, J. Huang, C. He, *Macromolecules* **2005**, *38*, 3554; b) H. Loc Nguyen, P. N. Horton, M. B. Hursthouse, A. C. Legon, D. W. Bruce, *J. Am. Chem. Soc.* **2004**, *126*, 16; c) P. Metrangolo, C. Präsang, G. Resnati, R. Liantonio, A. C. Whitwood, D. W. Bruce, *Chem. Commun.* **2006**, 3290.

[11] a) S. R. Batten, R. Robson, *Angew. Chem.* **1998**, *110*, 1558; *Angew. Chem. Int. Ed.* **1998**, *37*, 1460, and references therein; b) S. R. Batten, *CrystEngComm* **2001**, *3*, 67.

[12] a) V. A. Blatov, L. Carlucci, G. Ciani, D. M. Proserpio, *CrystEngComm* **2004**, *6*, 377; b) I. Baburin, V. A. Blatov, L. Carlucci, G. Ciani, D. M. Proserpio, *J. Solid State Chem.* **2005**, *178*, 2533; c) L. Carlucci, G. Ciani, D. M. Proserpio, in *Making Crystals by Design: Methods, Techniques and Applications* (Eds.: D. Braga, F. Grepioni), Wiley, New York, **2006**, Chapter 3.

[13] *Merck Index, Vol. 12*, Merck, Whitehouse Station, **1996**, p. 7245.

[14] a) Q. Wang, S. Mikkola, H. Lönnberg, *Tetrahedron Lett.* **2001**, *42*, 2735; b) A. Dupraz, P. Guy, C. Dupuy, *Tetrahedron Lett.* **1996**, *37*, 1237.

[15] a) S. P. Daffin, P. J. Duggan, S. A. M. Duggan, *Org. Lett.* **2001**, *3*, 917; b) Y. Ueno, M. Takeba, M. Mikawa, A. Matsuda, *J. Org. Chem.* **1999**, *64*, 1211; c) J. Esnault, J.-M. Mallet, Y. Zhang, P. Sinay, T. Le Bouar, F. Pincet, E. Perez, *Eur. J. Org. Chem.* **2001**, 253; d) B. Liu, R. Roy, *Chem. Commun.* **2002**, 594.

[16] N. Farcy, H. De Muynck, A. Madder, N. Hosten, P. J. De Clercq, *Org. Lett.* **2001**, *3*, 4299.

[17] a) X. Wang, M. Simard, J. D. Wuest, *J. Am. Chem. Soc.* **1994**, *116*, 12119; b) M. J. Zaworotko, *Chem. Soc. Rev.* **1994**, *23*, 283; c) J.-H. Fournier, T. Maris, J. D. Wuest, W. Guo, E. Galoppini, *J. Am. Chem. Soc.* **2003**, *125*, 1002; d) P. Brunet, M. Simard, J. D. Wuest, *J. Am. Chem. Soc.* **1997**, *119*, 2737; e) L. Vaillancourt, M. Simard, J. D. Wuest, *J. Org. Chem.* **1998**, *63*, 9746; f) D. Laliberté, T. Maris, P. E. Ryan, J. D. Wuest, *Cryst. Growth Des.* **2006**, *6*, 1335; g) S. V. Lindeman, J. Hecht, J. K. Kochi, *J. Am. Chem. Soc.* **2003**, *125*, 11597; h) P. Grosshans, A. Jouaiti, M. W. Hosseini, N. Kyritsakas, *New J. Chem.* **2003**, *27*, 793; i) K. I. Nättinen, K. Rissanen, *Inorg. Chem.* **2003**, *42*, 5126; j) K. I. Nättinen, P. E. N. de Bairos, P. J. Seppälä, K. T. Rissanen, *Eur. J. Inorg. Chem.* **2005**, 2819.

[18] a) D. S. Reddy, D. C. Craig, A. D. Rae, G. R. Desiraju, *J. Chem. Soc. Chem. Commun.* **1993**, 1737; b) R. Thaimattam, C. V. K. Sharma, A. Clearfield, G. R. Desiraju, *Cryst. Growth Des.* **2001**, *1*, 103.

[19] a) K. I. Nättinen, K. Rissanen, *Cryst. Growth Des.* **2003**, *3*, 339; b) H. Sauriat-Dorizon, T. Maris, J. D. Wuest, *J. Org. Chem.* **2003**, *68*, 240; c) A. Pegenau, X. H. Cheng, C. Tschierske, P. Göring, S. Diele, *New J. Chem.* **1999**, *23*, 465; d) H. Jiang, S. J. Lee, W. Lin, *J. Chem. Soc. Dalton Trans.* **2002**, 3429; e) H. Jiang, S. J. Lee, W. Lin, *Org. Lett.* **2002**, *4*, 2149; f) L. Cheng, J. A. Cox, *Chem. Mater.* **2002**, *14*, 6; g) S. Brownstein, M. Zhou, *Magn. Reson. Chem.* **2003**, *41*, 1041.

[20] E. C. Constable, C. E. Housecroft, M. Cattalini, D. Phillips, *New J. Chem.* **1998**, *22*, 193.

[21] a) C. St. Pourcain, A. Griffin, *Macromolecules* **1995**, *28*, 4116; b) K. N. Wiegel, A. C. Griffin, M. S. Black, D. A. Schiraldi, *J. Appl. Polym. Sci.* **2004**, *92*, 4097.

[22] M. T. Messina, P. Metrangolo, W. Navarrini, S. Radice, G. Resnati, G. Zerbi, *J. Mol. Struct.* **2000**, *524*, 87.

[23] T. Pilati, A. Forni, *J. Appl. Crystallogr.* **1998**, *31*, 503.

[24] L. Carlucci, G. Ciani, D. M. Proserpio, *Coord. Chem. Rev.* **2003**, *246*, 247.

[25] See http://www.chem.monash.edu.au/staff/sbatten/interpen/index.html; S. U. Son, B. Y. Kim, C. H. Choi, S. W. Lee, Y. S. Kim, Y. K. Chung, *Chem. Commun.* **2003**, 2528.

[26] a) L. Carlucci, G. Ciani, P. Macchi, D. M. Proserpio, S. Rizzato, *Chem. Eur. J.* **1999**, *5*, 237; b) L. Carlucci, G. Ciani, D. M. Proserpio, S. Rizzato, *Chem. Eur. J.* **2002**, *8*, 1519; c) L. Carlucci, G. Ciani, D. M. Proserpio, S. Rizzato, *CrystEngComm* **2002**, *4*, 413.

[27] D. S. Reddy, T. Dewa, K. Endo, Y. Aoyama, *Angew. Chem.* **2000**, *112*, 4436; *Angew. Chem. Int. Ed.* **2000**, *39*, 4266.

[28] Bruker, SMART, SAINT and SADABS, Bruker AXS Inc., Madison, Wisconsin (USA), **1999**.

[29] M. C. Burla, M. Camalli, B. Carrozzini, G. L. Cascarano, C. Giacovazzo, G. Polidori, R. Spagna, *J. Appl. Crystallogr.* **2003**, *36*, 1103.

[30] G. M. Sheldrick, SHELXL-97, Program for the Refinement of Crystal Structures, University of Göttingen, Göttingen (Germany), **1997**.

Received: November 17, 2006
Published online: April 3, 2007

